Clays and Clay Minerals, Vol. 54, No. 6, 703–720, 2006.

'BLACK' SOILS IN THE SOUTHERN ALPS: CLAY MINERAL FORMATION AND TRANSFORMATION, X-RAY AMORPHOUS Al PHASES AND Fe FORMS

R. Zanelli[1], M. Egli[1,*], A. Mirabella[2], M. Abdelmoula[3], M. Plötze[4] and M. Nötzli[1]

[1] Department of Geography, University of Zurich, CH-8057 Zurich, Switzerland
[2] ISSDS, Research Institute for Soil Study and Conservation, Firenze, Italy
[3] Laboratoire de Chimie Physique et Microbiologique pour l'Environnement (LCPME), UMR 7564 CNRS-UHP Nancy I, France
[4] ETH Zurich, Institute for Geotechnical Engineering, 8093 Zurich, Switzerland

Abstract—Many soils in southern Switzerland have a black color, contain a large amount of soil organic matter (SOM) and seem to have some andic properties although they did not develop on volcanic parent material. We investigated three typical 'black' soils to determine the mechanisms of (clay) mineral formation and transformation. We measured total element pools as well as the dithionite-, pyrophosphate- and oxalate-extractable fractions (Fe, Al, Si). The clay fraction (<2 μm) was analyzed using X-ray diffraction and FTIR spectroscopy. Iron speciation in the solid phase was determined by Mössbauer spectroscopy. With increasing weathering conditions, the plagioclase (albite) content decreases, trioctahedral species in the clay fraction such as biotite, chlorite or trioctahedral vermiculite either decompose or transform into a dioctahedral mineral such as dioctahedral vermiculite or hydroxy interlayered smectite (HIS). Typical weathering products were hydroxy interlayered vermiculite (HIV), HIS, interstratified minerals and kaolinite. The oxidation of Fe(II) into Fe(III) was evident and contributes to the transformation of trioctahedral mineral species into dioctahedral ones. In one soil, a large part of the Fe (up to 41%) was found in the form of Fe oxides. In the surface horizon, the poorly crystalline mineral ferrihydrite was dominant, while in the subsoil goethite prevailed. Maghemite (or maghemite/hematite mixture) was, furthermore, found in distinct concentrations down to a depth of ~50 cm. The formation of this mineral requires high temperatures which means that a forest fire can influence soil mineralogy down to a considerable depth. The specific climatic conditions with periods of strong humidity alternating with periods of winter droughts, sporadic fire events and the relatively large content of poorly crystalline fractions of Fe and Al contributed to the stabilization of SOM.

Key Words—Clays, Fe-speciation, Fire, Maghemite, Soil Minerals, Weathering.

INTRODUCTION

Soils of southern Switzerland are rich in organic carbon and often exhibit a black color. The organic C pools in these soils are generally very high when compared to other regions in the Alps (Blaser *et al.*, 1997). This kind of soil is usually found at sites <1000 m above sea level that are, in most cases, dominated by chestnut forest (*Castanea sativa*). However, the *Castanea sativa* species do not reflect the original forest vegetation and they were probably introduced by the Romans ~2000–3000 y ago. The colonization by the chestnut trees above the city of Ascona (between Losone and Arcegno) was dated to ~2000 y BP (Burga and Perret, 1998; Zoller, 1960). A more recent study (Schlumpf, 2004) suggests, however, that colonization had already occurred at ~3000 y BP.

Chestnut wood is rich in tannins. Soil organic matter (SOM) that contains tannins and other polymerized polyphenols is more resistant to microbial degradation (Williams and Gray, 1974; Zunino *et al.*, 1982). Furthermore, dissolved organic matter in aqueous extracts of chestnut leaves binds readily with Al, Fe and trace metals (Blaser and Sposito, 1987; Luster, 1990). The formation of organo-metallic complexes darkens the soil and strengthens the resistance of SOM to degradation (Blaser and Sposito, 1987; Boudot *et al.*, 1989; Blaser *et al.*, 1997). Blaser *et al.* (1997) hypothesized that the stability of SOM with its uniform dark color in cryptopodzolic soils in southern Switzerland can be explained as a combined effect of the chemical nature of the chestnut litter layer and the Al- and Fe-rich parent material. The very porous nature of the soils and the partially wet climate favor the transfer of dissolved organic carbon from the litter layer into the mineral soil and contribute to the thickness of the dark-colored horizons and the characteristic vertical distribution of SOM. Furthermore the cryptopodzolic soils described in southern Switzerland (Blaser *et al.*, 1997) differ in their chemistry and their relationship to environment from cryptopodzolic soils described elsewhere (*e.g.* De Coninck *et al.*, 1976; Duchaufour, 1976; Righi *et al.*, 1986). Differences exist in the C/N ratio, the leaching of organic matter and the distribution and mobility of Al and Fe in the soil. On one hand, the high precipitation during the growing period (527 mm, April–June) favors the leaching of dissolved organic matter to

* E-mail address of corresponding author:
megli@geo.unizh.ch
DOI: 10.1346/CCMN.2006.0540606

depth, whereas winter drought (180 mm, December–February) enhances polycondensation of the SOM and contributes to its stability. Newer findings, furthermore, suggest that charred organic carbon may increase the amount of aromatic C and contribute to a relatively inert type of SOM (Skjemstad *et al.*, 1996). There is evidence that charred organic carbon plays an important role in many soils worldwide such as Chernozems (*e.g.* Schmidt *et al.*, 1999), Argentinian Hapludolls (Zech *et al.*, 1997), Japanese volcanic ash soils (Golchin *et al.*, 1997), soils of the French Alps (Carcaillet and Talon, 2001), *etc.* Forest fires are common in southern Switzerland, although, at first glance, the climate has a wet character. The possibility exists, therefore, that as well as the mechanisms suggested by Blaser *et al.* (1997), fire could also have a noticeable influence on the accumulation of SOM and on the characteristics of clay minerals and X-ray amorphous phases.

Until now the clay minerals and X-ray amorphous phases of these soils have not been investigated. The question arises, therefore, of how these components have evolved under these local conditions. Although the soils in southern Switzerland are not developed on volcanic parent material they are suggested to have some common properties with volcanic soils such as the typical black A horizon in Andosols (Shindo *et al.*, 2002; Zehetner *et al.*, 2003) or the large amount of secondary Al and Fe phases. In this paper, emphasis is placed on the identification and detailed characterization of clay minerals and their formation and transformation reactions as well as on the detection of secondary Fe and Al phases. As fire has probably also affected the soil mineralogy, special attention has been given to the determination of Fe in clays and oxy-hydroxides.

MATERIALS AND METHODS

Study sites

We studied three typical 'black' soil profiles in southern Switzerland (Ticino) (Figure 1, Table 1). The climate is generally humid and moderate (mean annual precipitation is ~1700 mm for Locarno and the mean annual temperature is near 11.5ºC; EDI, 1992). Forest fires are common during the rather dry winter period. The springs and autumns are wet (June–September ~800 mm of precipitation), whereas the summers are sunny with sporadic thunderstorms.

The sites at Ascona I and Pura are dominated by the *Castanea sativa* species, while at Ascona II there is an older *Quercetum-Betuletum* vegetation (Table 1). The geology near Ascona, where two sites were selected, is dominated by gneissic glacial deposits (SGK, 1967; SGK, 1974) that include some eolian addition. Some inclusions of basic silicate rocks (amphibolite) occur occasionally. Gneissic parent material prevails at the site situated close to Pura (area of Lago di Lugano). As these sites were covered by ice during the last glaciation, weathering and soil formation could not have begun >20,000 y ago (Hantke, 1978, 1983). The parent material is probably of periglacial or late-glacial origin (cf. Mailänder and Veit, 2001), just before the reforestation (±15−13 ka BP) during Bölling.

Sampling

Soil profiles ditches were dug down to the C (BC) horizon. Soil samples of 1−2 kg were collected from each horizon. Soil bulk density was determined with a soil core sampler and undisturbed soil samples were taken down to the C (BC) horizon. The soils did not exhibit any signs of erosion and could be considered as natural.

Soil characteristics

Element pools in the soil (Ca, Mg, K, Na, Fe, Al, Mn, Si and Ti) were determined by the method of total dissolution. Oven-dried samples were dissolved using a mixture of HF, HCl, HNO_3 and H_3BO_3 as in Hossner (1996) and modified as in Fitze *et al.* (2000), in a closed system (microwave-oven and under high pressure, 25 bar). The elemental concentrations were determined by atomic absorption spectroscopy. Additionally, the dithionite-, pyrophosphate- and oxalate-extractable fractions were measured for the elements Fe, Al and Si (McKeague *et al.*, 1971). The extracts were centrifuged for 10 min at 4000 rpm and then filtered through a 0.45 µm filter (S&S, filtertype 030/20). Total C and N contents of the soil were measured with a C/N analyzer (Elementar Vario EL). The soil pH (in 0.01 M $CaCl_2$)

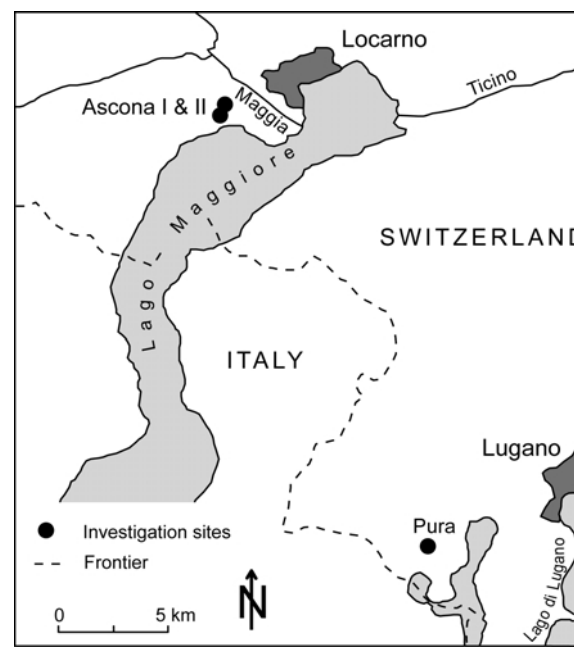

Figure 1. Locations of the investigation sites in southern Switzerland.

Table 1. Site characteristics.

Site	Coordinates	Altitude (m above sea level)	Exposure	Slope (%)	Dominant vegetation	Soil type (WRB, 1998)	Geological substrate
Pura	45º98′50″ N 8º86′24″ E	650	SW	22	*Castanea sativa*, *Fagus silvatica*, *Quercus sp.*	Humic Umbrisol	Granite, orthogneiss
Ascona I	46º09′32″ N 8º45′27″ E	360	SE	10	*Castanea sativa*	Andosol? Humic Umbrisol	Gneissic moraine deposits on gneissic and amphibolitic ribs
Ascona II	46º09′29″ N 8º45′24″ E	340	SE	5–10	*Quercetum-Betuletum Polgonatum multiflorum Populus tremula Prunus avium*	Humic Umbrisol	Gneissic moraine deposits on gneissic and amphibolitic ribs

was determined on the fine-earth fraction of air-dried samples using a soil:solution ratio of 1:2.5.

After pretreatment of the samples with H_2O_2 (3%), the particle-size distribution of the soils was measured by a combined method consisting of sieving the coarser particles (2000−32 μm) and the measurement of the finer particles (<32 μm) by means of an X-ray sedimentometer (SediGraph5100).

Soil mineralogy

The clay fraction (<2 μm) was obtained from the soil after destruction of organic matter with dilute and Na acetate-buffered H_2O_2 (pH 5) by dispersion with Calgon and sedimentation in water (Egli *et al.*, 2001). Oriented specimens on glass slides were analyzed by X-ray diffraction (XRD) (3 kW Rigaku D/MAX III C diffractometer, equipped with a horizontal goniometer and a curved-beam graphite monochromator) using CuKα radiation from 2 to 15º2θ with steps of 0.02º2θ at 2 s per step. The following treatments were performed: Mg saturation, ethylene glycol solvation (EG) and K saturation, followed by heating for 2 h at 335 and 550ºC. Sodium citrate treatment was performed to extract interlayered hydroxy-Al (or Fe) contaminants. We applied a modified procedure according to Tamura (1958), in which the heating of the samples was performed in an autoclave at 135ºC with a contact time of 24 h without extractant removal (Carnicelli *et al.*, 1997). The Na citrate-treated clays were Mg saturated, solvated with ethylene glycol, K saturated and heated at 335 and 550ºC for 2 h. The XRD patterns of the Na citrate-treated samples were then compared with those of the corresponding untreated samples. The collapse of the hydroxy interlayered 2:1 clay minerals is greatly improved after the removal of the interlayers and K saturation. Furthermore, the presence of HIS (hydroxy interlayered smectites) is demonstrated by a more pronounced peak at 1.65 nm following ethylene glycol solvation.

The d_{060} region was studied on random mounts prepared by back-filling Al holders and gently pressing over filter paper and then step-scanned from 58 to 64º2θ with steps of 0.02º2θ at 10 s intervals. Digitized X-ray data were smoothed and corrected for Lorentz and polarization factors (Moore and Reynolds, 1997). Peak separation and profile analysis were carried out with the Origin PFM™ using the Pearson VII function after smoothing the diffraction patterns by a Fourier transform function. Background values were calculated by means of a non-linear function (polynomial 2nd order function; Lanson, 1997).

The quantitative mineralogical composition of the inorganic part of the fine earth fraction (<2 mm) was characterized using the 'Rietveld analyse' (program AutoQuan, GE SEIFERT) on XRD patterns of randomly orientated specimens (Philips PW1820; CuKα, 40 kV, 30 mA 4−70º2θ, steps of 0.02º2θ, 3 s per step,

automatic slits) (Bergmann *et al.*, 1998; Bergmann and Kleeberg, 1998).

Imogolite-type material (ITM), meaning the sum of imogolite and proto-imogolite allophane, was estimated (assuming that the Al/Si molar ratio is close to 2.0) according to Parfitt and Henmi (1982), i.e. as allophane + imogolite% = Si(oxalate)% · 7.1. The presence of ITM and kaolinite was checked with FTIR measurements. Spectra were recorded over the range of 4000 to 250 cm^{-1} on pellets made with 1 mg of sample and 250 mg of KBr that had previously been heated at 150ºC. The ITM was further investigated by determining the molar ratio $(Al_o - Al_p)/Si_o$ with Al_o as the oxalate-extractable Al, Al_p as the pyrophosphate-extractable Al and Si_o as the oxalate-extractable Si.

Determination of the layer charge of expandable clay minerals in the soil

Layer-charge estimation was performed using the long-chain alkylammonium ion C18 according to the method proposed by Olis *et al.* (1990).

For the monolayer to bilayer transition, equation 1 was used:

$$d_{001} = 8.21 + 34.22\xi \quad (1)$$

with ξ = mean layer charge and *d* values given in Å. For the bilayer to pseudotrimolecular layer transition, the equation is:

$$d_{001} = 8.71 + 29.65\xi \quad (2)$$

Values of layer charge calculated from *d* spacings >3.1 nm are beyond the limits of the C-18 BTP regression model of Olis *et al.* (1990) and, therefore, will be indicated as >0.75 per half unit-cell.

Determination of Fe forms in the soil

The ^{57}Fe Mössbauer spectroscopy of environmental materials has been mainly concerned with Fe in clay minerals and oxides. A distinction of Fe in these two groups is relatively straightforward: the phyllosilicates are paramagnetic at room temperature and may contain both divalent and trivalent Fe, whereas the most common Fe oxides should be magnetically ordered and contain only trivalent Fe (Murad, 1998; Guillaume, 2003). When distinct Fe species are present in a solid material, the relative structural areas of the subspectra associated with these species are proportional to their relative abundances.

Transmission Mössbauer spectra were collected using a constant-acceleration spectrometer with a 50-mCi source of ^{57}Co in Rh. The spectrometer was calibrated with a 25 μm foil of α-Fe at room temperature. The cryostat consisted of a closed-cycle helium Mössbauer cryogenic workstation with a vibrations isolation stand manufactured by Cryo Industries of America. Helium exchange gas was used to thermally couple the sample to the refrigerator, allowing variable temperature operation from 12 to 300 K. All measurements were performed with a large velocity range of ±11 mm s^{-1} in order to detect the magnetically split components of the samples. The spectra were fitted with a standard Lorentzian multiplet analysis and/or the Voigt-based fitting method when needed, as implemented in the Recoil software of Lagarec and Rancourt (University of Ottawa, Canada).

RESULTS

Soil characteristics

The soils develop on siliceous parent material and can be classified as Humic Umbrisols (Table 1). However, the soils also show some andic properties which will be discussed later. All soils from the investigation areas have a sandy to silty texture. However, there were noticeable differences in the particle-size distribution between the sites. The parent materials of Ascona I and II contain up to 80% silt and of Pura only ~20%. The soil skeleton and the silty-sandy texture generally lead to a high degree of water permeability in the soils. For Pura and Ascona II, the clay contents are, at most, 59 and 77 g kg^{-1}, respectively (Table 2). The acidification of the soils, due to their gneissic parent material, is pronounced, with pH values in the topsoils ranging between 3.45 and 4.0. The profiles showed noticeably dark-colored horizons down to 65 cm (Ascona II). Organic matter is obviously incorporated deep into the soil and a large organic matter content was measured in all topsoils (total C content between 11.6% and 13.4%). The C/N ratio in the topsoil varies between 17 and 22 (Table 2). The levels of extractable Al and Fe contents (dithionite, oxalate and pyrophosphate) were rather high. All soil profiles showed an early stage of podzolization where the translocation of X-ray amorphous Al and Si in the soil profile seems incipient, although no mobilization of X-ray amorphous Fe and organic matter was observed (Table 3).

The main geochemical data of the soil and parent material is given in Table 4. The composition of the investigated material primarily reflects the Si-rich and gneissic character. There are minor differences in the chemical composition of the C horizons between the sites, especially with respect to the MgO and Fe_2O_3 content.

Mineral quantification

Total content and AUTOQUAN analysis of the fine-earth fraction (<2 mm) showed, for the soil profiles in Ascona, a rather Si-rich composition, with large quartz and feldspar contents (Table 6). The fine earth of the profile at Ascona I had a higher mica and a slightly lower plagioclase (albite) content. In contrast to mica, the concentration of chlorite between the profiles did not differ greatly. Both profiles were taken close to each other on glacial deposits. A small heterogeneity in the parent material is obvious. Both profiles contain

Table 2. Some chemical and physical properties of the fine earth (<2 mm) of the investigated soils.

Site/ horizon	Soil depth (cm)	Sand (g kg^{-1})	Silt (g kg^{-1})	Clay (g kg^{-1})	Skeleton (g kg^{-1})	Bulk density (g cm^{-3})	pH ($CaCl_2$)	N (g kg^{-1})	C (g kg^{-1})	C/N
Ascona I										
Ah1	0–20	13	829	159	5	0.55	4.0	7.0	134.3	19.2
Ah2	20–45				14	0.57	4.2	4.5	99.8	22.3
Bw	45–85				4	0.91	4.6	1.1	24.6	23.2
BC	85–135	29	840	147	91	1.13	5.0	0.6	12.9	20.2
Ascona II										
Ah1	0–25	377	564	59	217	0.65	4.0	5.6	116.2	20.9
Ah2	25–55				370	0.87	4.4	2.7	61.7	22.9
Bw	55–80				534	1.36	4.9	0.5	13.1	29.0
BC	80–110	131	837	32	362	1.37	4.9	0.2	6.9	29.8
Pura										
Ah	0–13				19	0.59	3.45	6.91	119.1	17.2
A(E)	13–30	703	220	77	38		4.36	4.49	87.5	19.5
Bh1	30–40				57			3.10	65.6	21.2
Bh2	40–50	753	184	63	69	0.82	4.63	2.21	44.3	20.0
Bw	50–68	739	177	84	206	1.26	5.03	1.22	21.3	17.5
Cw	>68	720	222	58			5.14	0.24	5.8	24.1

Table 3. Dithionite- (d), oxalate- (o) and pyrophosphate- (p) extractable Al, Fe and Si and calculated ITM contents in the soils.

Site	Soil depth (cm)	Al_d (g kg^{-1})	Al_o (g kg^{-1})	Al_p (g kg^{-1})	Si_o (g kg^{-1})	Fe_d (g kg^{-1})	Fe_o (g kg^{-1})	Fe_p (g kg^{-1})	Fe_d-Fe_o (g kg^{-1})	ITM (%)	Molar ratio $(Al_o-Al_p)/Si_o$	Al_o+1/2 Fe_o (%)
Ascona I												
Ah1	0–20	14.51	10.62	12.98	0.192	22.04	14.02	15.19	8.02	0.1	−12.28	1.76
Ah2	20–45	20.05	17.26	18.68	1.233	19.19	11.71	12.67	7.47	0.9	−1.15	2.31
Bw	45–85	9.94	11.75	5.71	4.349	11.57	3.43	1.27	8.14	3.1	1.39	1.35
BC	85–135	8.01	12.52	3.39	5.522	6.65	2.23	0.50	4.42	3.9	1.65	1.36
Ascona II												
Ah1	0–25	12.96	11.26	11.61	0.384	7.95	4.63	4.78	3.32	0.3	−0.90	1.36
Ah2	25–55	14.16	12.33	12.03	1.810	8.76	4.70	4.35	4.06	1.3	0.16	1.47
Bw	55–80	6.88	9.33	3.42	4.169	4.02	1.73	0.41	2.28	3.0	1.42	1.02
BC	80–110	4.38	6.79	2.05	3.118	2.35	1.28	0.27	1.08	2.2	1.52	0.74
Pura												
Ah	0–13	6.37	6.16	8.68	0.075	11.63	7.92	12.13	*	0.053	−35.03	1.01
A(E)	13–30	14.60	10.44	14.08	0.335	12.33	5.84	9.47	*	0.237	−11.31	1.34
Bh2	40–50	13.24	11.70	10.19	2.212	12.57	4.47	6.01	8.10	1.570	0.71	1.32
Bw	50–68	9.04	11.42	5.16	3.396	10.77	3.57	1.90	7.20	2.411	1.92	0.59
Cw	>68	3.79	5.37	1.95	1.770	5.37	1.16	0.35	4.21	1.257	2.01	1.01

* not determined because of the high pyrophosphate-extractable Fe content

hornblende with a tendency to decrease towards the soil surface. In the Ascona I but also in Ascona II soil profiles, a decrease in plagioclase towards the surface horizons could be detected, while the K-feldspar content seemed to be more or less stable. The BC horizon of Ascona II differed from the other horizons and was characterized by a higher quartz and plagioclase, but a lower K-feldspar content.

Clay mineralogy

Ascona I and II. The clay mineralogy of both these profiles showed some similarities. The Mg-saturated samples of the BC horizon gave peaks at 1.4, 1.20, 1.0 and 0.71 nm. With increasing weathering, the peak at 1.2 nm decreases strongly. This peak persists after EG solvation and K saturation. Only heating to 335ºC led to its collapse to 1.0 nm. Therefore, it could be attributed to an interstratified mica-HIV mineral. The Mg-saturated and ethylene glycol-solvated samples gave similar XRD patterns. Smectite was therefore virtually absent from the clay fraction or present only in traces. The main part of the peak at 1.40 nm collapsed to 1.0 nm following K saturation and heating at 335ºC and consequently was assigned to a hydroxy interlayered vermiculite (HIV); the residual peak retained its position, even after the heating treatment at 550ºC and, therefore, belongs to chlorite (Figure 2). Chlorite was present in all soils in the C horizon. In some cases, chlorite had similarities to a highly hydroxy interlayered mineral (reduction of the peak at 1.4 nm after heating at 550ºC with Na citrate treatment).

The Na citrate-treated clays (Figure 3) of the topsoils showed a distinct peak near 1.65–1.66 nm in the XRD pattern of the EG-solvated sample that is due to hydroxy interlayered smectite (HIS) that has transformed into smectite following the removal of the hydroxy interlayer. A smaller peak (when compared to the untreated sample) was still present at 1.4 nm after heating to 550ºC. A part of the chlorite (identified in the untreated sample) collapsed to 1.0 nm following the citrate treatment and heating at 550ºC. This type of chlorite seems, therefore, to be present in a weathered state because it contains removable hydroxy interlayers. Towards the topsoil, a decrease in mica and mainly in mica-HIV mixed-layered minerals was measurable. In contrast to this tendency, more kaolinite (with respect to an increased FTIR adsorption-band intensity at 3695 cm^{-1}) was detectable (Figure 4). At Ascona I, soil weathering seemed to be more pronounced, due to a distinct lower concentration of mica-HIV mixed-layered minerals in the subsoil when compared to Ascona II.

Pura. The clays in the profile of Pura did not differ greatly from the other two soils. The Mg-saturated clay sample of the Cw horizon exhibited peaks at 1.40, 1.18, 1.00 and 0.71 nm. Almost no changes were measurable after EG solvation and K saturation. No expandable

Table 4. Total fine earth contents of some horizons of the investigated soils.

Site/ horizon	Depth (cm)	SOM* (g kg^{-1})	Al_2O_3 (g kg^{-1})	Fe_2O_3 (g kg^{-1})	SiO_2 (g kg^{-1})	TiO_2 (g kg^{-1})	CaO (g kg^{-1})	MgO (g kg^{-1})	K_2O (g kg^{-1})	Na_2O (g kg^{-1})	MnO (g kg^{-1})	IVC† (g kg^{-1})	Total (g kg^{-1})
Ascona I													
Ah1	0–20	231.0	116.4	47.5	447.1	8.8	6.9	8.8	12.5	9.0	0.4	100.9	989.4
Ah2	20–45	171.6	137.8	46.3	468.0	9.1	8.2	10.6	18.2	10.2	0.5	101.0	981.5
Bw1	45–85	42.3	158.5	49.8	576.2	10.7	11.9	23.2	20.9	7.6	0.8	74.3	976.1
BC	85–135	22.3	159.5	50.6	593.4	8.3	11.3	17.8	20.6	19.2	1.0	65.9	969.8
Ascona II													
Ah1	0–25	199.9	116.9	33.3	484.4	6.1	10.1	11.3	15.8	15.4	0.6	85.4	979.3
Ah2	25–55	106.1	140.6	32.8	539.0	7.9	7.8	12.0	16.9	18.3	0.7	74.4	956.5
Bw	55–80	22.4	152.0	41.0	598.6	8.2	15.6	16.2	18.9	45.7	0.8	53.9	973.4
BC	80–110	11.8	140.9	28.5	678.0	9.1	13.4	12.7	23.4	25.8	0.7	33.3	977.5
Pura													
A(E)	13–30	202.5	117.5	34.0	592.7	6.7	5.5	7.1	19.0	10.4	n.d.	33.5	1028.9
Cw	>68	9.9	149.0	33.1	724.9	5.8	9.1	8.5	27.8	21.7	n.d.	34.1	1023.9

* Soil organic matter (organic C × 1.72). † inorganic volatile compounds, estimated by loss on ignition from soil organic matter
n.d. not determined

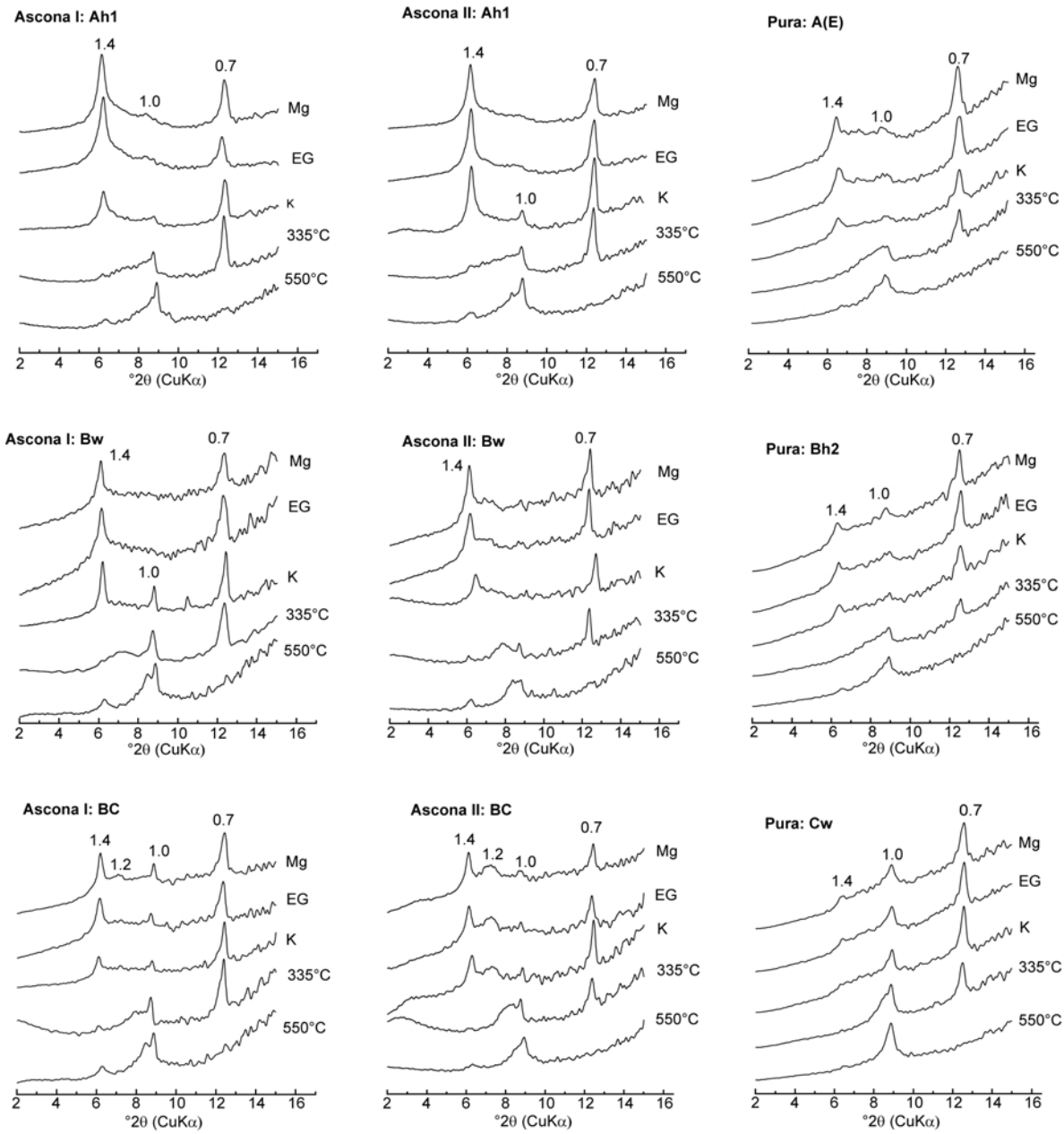

Figure 2. XRD patterns of the <2 μm fraction from all profiles. The curves are smoothed and corrected for Lorentz and polarization factors. *d* spacings are given in nm.

minerals and no vermiculite are, therefore, present in the C horizon. The peak at 1.18−1.15 nm maintained its position following K saturation, indicating the presence of interstratified mica-HIV. With decreasing soil depth (Bh2 and A(E) horizons) the mica peak decreases strongly when compared to the parent material and, correspondingly, the peak at 1.39 nm (HIV) increases. Mixed-layered mica-HIV and chlorite are still present. According to the FTIR analyses, the soil contained kaolinite throughout the whole profile (*cf.* Figure 4).

An overview of the clay minerals determined for each profile is given in Table 5.

Dioctahedral and trioctahedral structures

The d_{060} reflections of the clays are shown in Figure 5. In all subsoils, substantial amounts of trioctahedral species could be measured. The trioctahedral species (given by the peaks in the region 0.1528−0.1538 and 0.1544 nm; Fanning *et al.*, 1989; Moore and Reynolds, 1997) decrease towards the soil surface while the dioctahedral ones increase. In contrast to the other profiles, the surface soil of Ascona I had only traces of trioctahedral clay species given by the peaks at 0.1499−0.1490 nm. Mica, indicated by a peak at 1.0 nm, is present in moderate concentration. Therefore, mica in

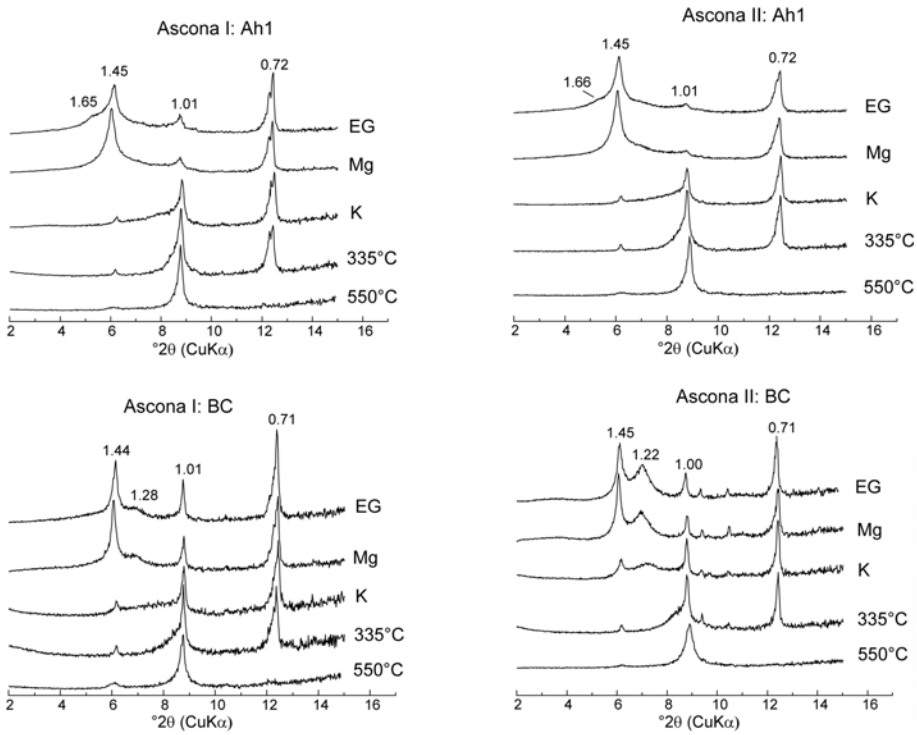

Figure 3. XRD patterns of the <2 μm fraction treated with Na citrate, from Ascona I and II. The curves are smoothed and corrected for Lorentz and polarization factors. *d* spacings are given in nm.

the surface horizon of soil profile Ascona I should be dioctahedral and could be muscovite that seems to be more resistant to weathering processes. Regarding the d_{060} reflections, the decrease in trioctahedral species is mainly due to the transformation of trioctahedral species such as mica (biotite) and chlorite to dioctahedral species (such as HIV, HIS, interstratified mica-HIV).

Layer charge

The layer charge of mineral species was differentiated with the alkylammonium method (C18) (Olis *et al.*, 1990) on Na citrate-treated clay samples. Distinct peaks in the XRD patterns at 1.84, 1.65 and 3.74 nm could be detected (data not shown) in the surface horizons of the soils. The peak at 3.74 nm was beyond the limits of the C-18 BTP regression model of Olis *et al.* (1990) and, therefore, will be indicated as >0.75 per half unit-cell and corresponds to the high-charged clay mineral vemiculite. The peak at 1.84 nm could be a d_{002} reflection of the peak at 3.74 nm and probably belongs to the same high-charged clay mineral. The peak at 1.65 nm could be attributed to a lower-charged clay mineral with a mean layer charge per half unit-cell of ~0.3. This low-charged clay mineral corresponds to a smectitic phase. Both vermiculite and smectite contain mostly hydroxy interlayers. Therefore, the samples contain HIV and HIS instead of vermiculite and smectite, respectively. Towards the surface, a relative increase in low charges (and consequently of HIS) is measurable.

Imogolite-type material

Imogolite-type material was present in significant amounts in the subsoil of all profiles (Table 3 and Figure 4). The content was calculated according to Parfitt and Hemni (1982). The values of the ITM content vary in the subsoil between 1.4 and 3.9%, with the highest concentration in the BC horizon of the soil profile Ascona I. The band at 3695 cm^{-1} in the FTIR spectrum was assigned to kaolinite. Kaolinite has additional peaks in the 600–250 cm^{-1} region and some of them coincide with allophane and imogolite (*e.g.* at 348 cm^{-1}). The peak near 348 cm^{-1} could be partially due to ITM but taking the band at 3695 cm^{-1} into consideration for the samples Bh2 and Cw of Pura and Bw and BC of Ascona I and II, the peak must also be attributed to kaolinite. The Al/Si molar ratio for the same samples is between 1 and 2 indicating the presence of Si-rich ITM.

Fe phases and forms

With respect to the Fe phases, there are distinct differences between the profiles analyzed. At the site Ascona I, the most crystalline Fe oxyhydroxide (calculated by the difference between the Fe_d and Fe_o content) and total Fe content could be measured (Tables 3 and 4).

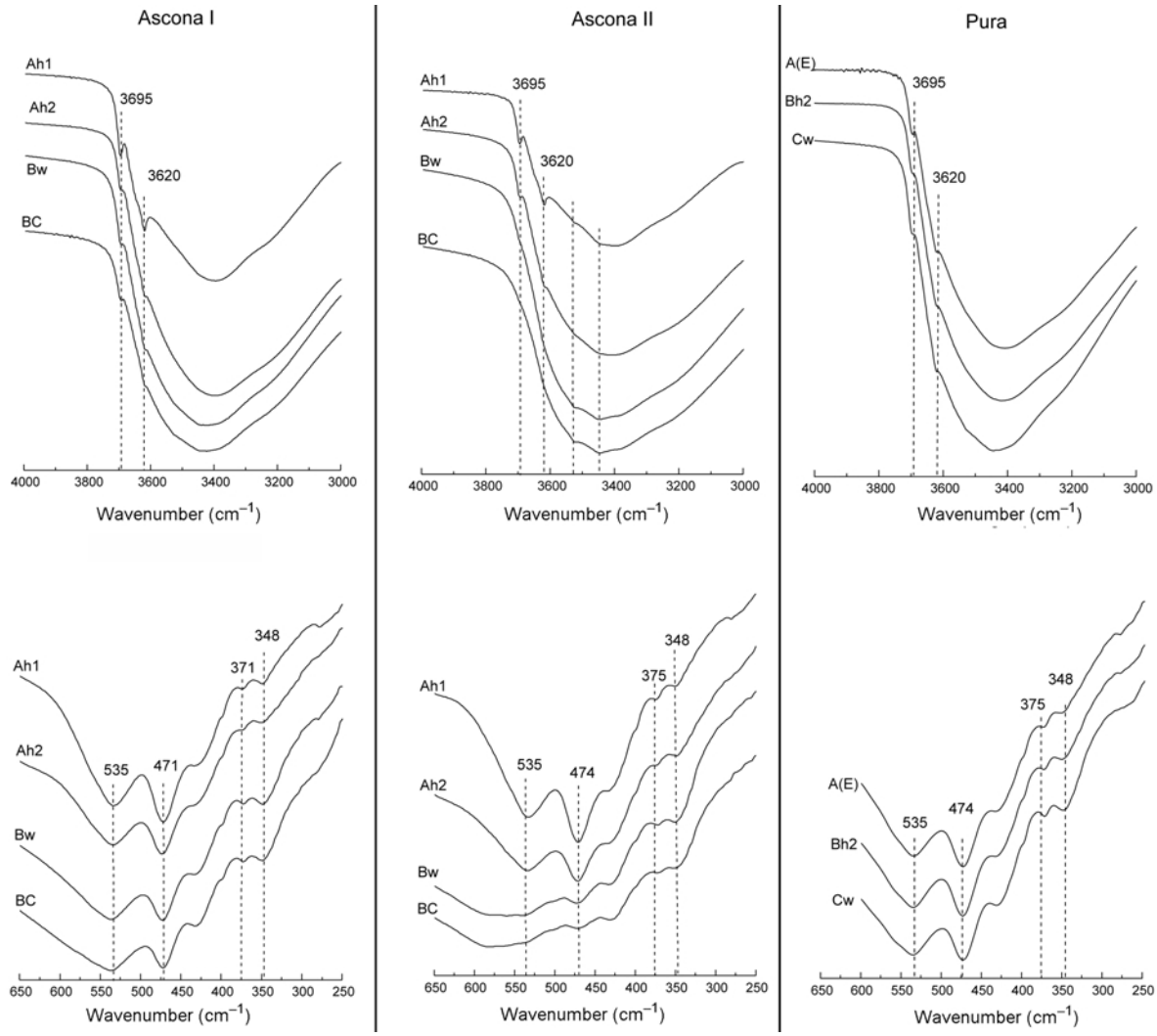

Figure 4. FTIR spectra of the soil clay fraction (<2 μm).

Mössbauer spectroscopy was carried out to obtain additional information about the Fe speciation in solid phases (Figure 6) and was performed for the two most contrasting profiles (on the basis of Fe chemistry). While at Ascona II most Fe in the solid fraction was chemically bound in silicate material (clays), the profile at Ascona I had a significant amount of Fe in the form of oxides (Table 7).

At the Ascona I site, a higher Fe(II) content in the subsoil was measured when compared to the surface horizon. A similar trend also exists at the Ascona II site. The oxidation of Fe(II) to Fe(III) could at least partially explain the transformation of tri- to dioctahedral clay minerals towards the surface. The speciation of Fe shows distinct differences between the sites Ascona I and II. At Ascona I, a considerable amount of Fe was found in the form of Fe oxides (Table 7). In the surface soil, 32% of solid Fe was present in the form of the poorly crystalline mineral ferrihydrite, while in the subsoil goethite prevailed. The large SOM content probably hindered the formation of more crystalline Fe oxides (Schwertmann, 1988). In the subsoil, where the SOM content was lower, the crystalline goethite was dominant. We detected, furthermore, the Fe oxide maghemite (or maghemite/hematite mixture) in the Ah1, Ah2 and Bw horizons of the Ascona I soil profile (down to a depth of 45–85 cm).

DISCUSSION

Soil chemical characteristics

The soils showed an early stage of podzolization with a slight translocation of Al within the profile, less evident for Fe (measurable at only the Pura site; Table 3). The more intense eluviation and illuviation process at Pura might be due to the greater permeability at this site (larger sand content).

Table 5. Clay mineral assemblages of the investigated soils.

Site/ horizon	Soil depth (cm)	Smectite	HIS	Vermiculite	HIV	Chlorite	Mica	Mica/HIV	Kaolinite	ITM
Ascona I										
Ah1	0–20	(X)	XX	XX	XX	X	XX	(X)	XX	
Ah2	20–45	(X)	XX	(X)	XX	X	X	X	X	
Bw	45–85		X	XX	XX	X	XX	X	X	XX
BC	85–135			X	XX	X	XX	XX	X	XX
Ascona II										
Ah1	0–25	(X)	XX	XX	XX	X	X	X	XX	
Ah2	25–55		(X)	(X)	XX	X	XX	X	X	
Bw	55–80			(X)	XX	X	XX	XX	(X)	XX
BC	80–110			X	XX	X	XX	XX		XX
Pura										
Ah	0–13									
A(E)	13–30			(X)	XX	X	XX	XX	XX	
Bh1	30–40									
Bh2	40–50			(X)	XX	X	XX	XX	X	(X)
Bw	50–68									
Cw	>68			(X)	XX	X	XX	XX	X	XX

XX = significant concentration, X = moderate concentration, (X) = traces

In the topsoil, the pyrophosphate-extractable Fe, Al and Si content exceeds the oxalate-extractable one. Fe and Al extracted by pyrophosphate are strongly associated with SOM (correlation of Al_p with SOM: R = 0.81; p <0.01; Fe_p with SOM: R = 0.90, p >0.01). As reported by Kaiser and Zech (1996), pyrophosphate may extract not only organically bound fractions but also coatings of $Al(OH)_3$ and peptized Al hydroxides associated with adsorbed organic matter. Compared to the oxalate extraction, higher pyrophosphate-extractable contents have been reported by other authors. Kleber *et al.* (2004) presumed that the alkaline pyrophosphate extractant attacks hydroxy-like Al (*e.g.* Al interlayers or poorly ordered gibbsite). Mizota and van Reeuwijk (1989) suggested dispersion problems and doubted the ability of the oxalate to completely dissolve strong humus-metal complexes. In our case we presume that Al was at least partially bound in humus-metal complexes and in peptized Al hydroxides associated with organic matter that were better dissolved in the alkaline (pH = 10) pyrophosphate than in the acid (pH = 3) oxalate extraction solution. Pyrophosphate probably also has extracted non-organic Fe forms. Ratios of organic carbon to Fe_p <10 indicate the (partial) dispersion of non-organic Fe. With the help of Mössbauer spectroscopy, Parfitt and Childs (1988) could show that Fe_p can be related to several particular forms in soils such as goethite or ferrihydrite that may be dispersed by pyrophosphate.

The soil profiles showed, furthermore, an early stage of podzolization. The translocation of X-ray amorphous (organic bound) Al and Si seemed to be incipient. Formation of ITM in the subsoil could be identified.

Table 6. Main mineral components contents (<2 mm), calculated by AUTOQUAN, standardized to the inorganic part.

Site/ horizon	Depth (cm)	Quartz (g kg^{-1})	K-feldspar (g kg^{-1})	Plagioclase (albite) (g kg^{-1})	(Na,Ca) hornblende (g kg^{-1})	Chlorite/HIV (g kg^{-1})	Mica (g kg^{-1})
Ascona I							
Ah1	0–20	447±16	114±13	171±13	43±12	87±11	139±13
Ah2	20–45	453±16	122±14	190±14	55±12	50±10	129±13
Bw1	45–85	391±15	127±14	234±13	53±12	57±12	139±13
BC	85–135	377±15	123±15	266±14	52±9	70±13	112±13
Ascona II							
Ah1	0–25	428±25	132±21	257±21	33±16	83±14	68±18
Ah2	25–55	434±24	131±20	259±21	39±16	44±16	93±20
Bw	55–80	425±17	122±18	287±16	33±11	68±8	65±15
BC	80–110	476±20	75±16	301±18	19±6	79±20	51±11

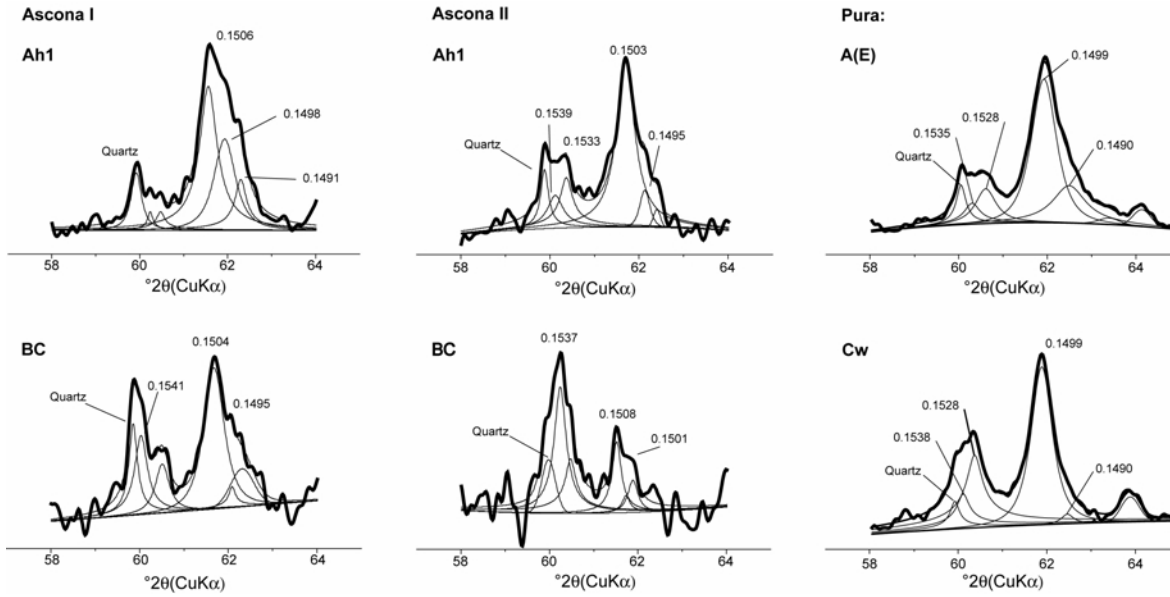

Figure 5. Peak separation of XRD patterns in the d_{060} region. *d* spacings are given in nm.

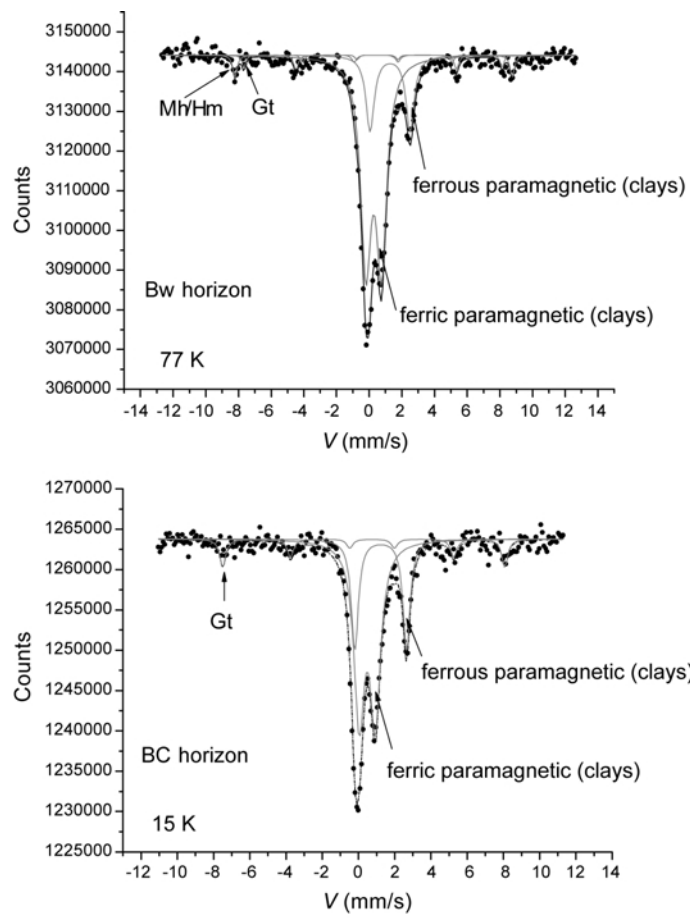

Figure 6. Mössbauer spectra of samples from Ascona I. Solid lines show individual fitting of components and their sum. Gt is assigned to goethite, Mh/Hm to hematite/maghemite mixtures.

Table 7. Relative fraction of solid Fe of the fine earth (<2 mm, in total Fe%) and hyperfine parameters of Mössbauer spectroscopy.

Characteristic	Site/ horizon	Soil depth, parameter	Goethite	Ferrihydrite	Maghemite/ hematite	Paramagnetic ferrous silicates (clays), Fe(II)	Paramagnetic ferric silicates (clays), Fe(III)
Relative abundance (%)							
	Ascona I						
	Ah1	0–20 cm		32	9	16	43
	Ah2	20–45 cm		11	17	26	46
	Bw	45–85 cm	3		6	21	70
	BC	85–135 cm	12			26	62
	Ascona II						
	Ah1	0–25 cm				20.5	79.5
	Ah2	25–55 cm				n.d.	n.d
	Bw	55–80 cm				n.d.	n.d.
	BC	80–110 cm				36 (30 + 6)	64
Hyperfine parameters							
	Ascona I						
	Ah1 (at 15 K)	CS (mm)		0.45	0.49	1.49	0.43
		Δ or ε (mm/s)		−0.07	0	2.54	0.98
		H (kOe)		477	528		
	Ah2 (at 15 K)	CS (mm)		0.45	0.37	1.21	0.45
		Δ or ε (mm/s)		0.08	0.04	2.65	0.92
		H (kOe)		471	529		
	Bw (at 77 K)	CS (mm)	0.5		0.47	1.4	0.4
		Δ or ε (mm/s)	−0.14		−0.078	2.45	0.95
		H (kOe)	490		526		
	BC (at 15 K)	CS (mm)	0.52			2.33	0.48
		Δ or ε (mm/s)	−0.23			2.85	0.88
		H (kOe)	483				
	Ascona II						
	Ah1 (at 77 K)	CS (mm)				1.2	0.45
		Δ or ε (mm/s)				2.88	0.79
		H (kOe)					
	BC (at 77 K)	CS (mm)				1.09; 0.95	0.33
		Δ or ε (mm/s)				2.65; 1.79	0.79
		H (kOe)					

CS = center shift
Δ or ε: quadrupole splitting or quadrupole shift
H: hyperfine field

Clay and soil minerals

Dominant processes in the <2 mm fraction include the chemical breakdown of plagioclase (albite) with the consequent decrease and a slight enrichment of quartz towards the soil surface. The destabilization of plagioclase and mica leads to the formation of kaolinite, vermiculite and/or interlayered 2:1 type minerals (Bouchard and Jolicoeur, 2000). The slight decrease in hornblende from the parent material towards the surface horizon in the Ascona I profile may also contribute to the formation of kaolinite (Schroeder *et al.*, 2000) or smectitic components (Dreher and Niederbudde, 2000). No clear trends could be measured for the other main minerals in the <2 mm fraction.

In all profiles, the mica content in the clay fraction decreased from the C to the A horizon. Towards the topsoil, and therefore with increasing weathering, mica was transformed into vermiculite or dissolved. Interstratified mica-vermiculite/HIV and mica-HIS are a transitory weathering product of mica transformation into vermiculite and smectite, respectively. Regarding the d_{060} reflectance, a strong reduction in trioctahedral and a consequent increase in dioctahedral species was measured. As the stage of weathering proceeds, trioctahedral species such as biotite, chlorite or trioctahedral vermiculite were transformed into dioctahedral ones (*e.g.* dioctahedral vermiculite, HIS). The oxidation of Fe(II) into Fe(III) was ascertained and contributes to the transformation of trioctahedral mineral species into dioctahedral ones. Dioctahedral micaceous minerals can, however, be much more resistant (cf. Mirabella *et al.*, 2002). The HIS and some minor smectite contents in the topsoils indicated advanced weathering conditions. In Alpine soils, smectite is often the end-product of weathering in strongly leached and acidified horizons (Righi *et al.*, 1999; Mirabella and Egli, 2003; Egli *et al.*, 2003). Major mechanisms involved in podzolization include the production of low molecular weight organic acids that form soluble complexes with Al and Fe (Lundström *et al.*, 2000a, 2000b). The combination of rainfall and temperature and the presence of low molecular weight organic acids determine the removal of Fe and Al polymers from the interlayers of expandable minerals (Mirabella and Sartori, 1998; Lundström *et al.*, 2000b; Egli *et al.*, 2001). It is likely that the smectitic components (such as HIS) derive from chlorite, through the removal of hydroxy polymers, while mica weathers in a first step to regularly or irregularly interstratified mica-vermiculite clay minerals (Dahlgren *et al.*, 1993; Righi *et al.*, 1999; Egli *et al.*, 2001; Mirabella *et al.*, 2002). Increasing weathering conditions led to a decrease in the layer charge. The reduction in the charge of 2:1 clay minerals is a process that occurs before HIS will develop into smectite and, thus, before hydroxy polymers will be removed by low molecular weight organic acids (Mirabella and Egli, 2003).

Fire and Fe minerals

Heating of ferrihydrite or goethite may lead to the formation of maghemite (Nørnberg *et al.*, 2004). The presence of a significant amount of organic matter in the soil is one prerequisite for maghemite formation from goethite with heating (van der Marel, 1951; Stanjek, 1987; Ketterings *et al.*, 2000). The decrease in goethite towards the soil surface points to such a process. Ferrihydrite, however, could have been the original precipitate (instead of goethite in the surface horizons) due to the presence of organic matter. In southern Switzerland, forest fires are common so that they could cause the formation of maghemite (or maghemite/hematite mixture). Paleobotanical results suggest that fire had a tremendous influence on the development of the vegetation in that region (Tinner *et al.*, 1999).

In the soil profile at Ascona I, we found some charcoal that confirms fire activity. Maghemite (or maghemite/hematite) was found to a considerable depth (45−85 cm). Downward migration of Fe and, thus, maghemite (or maghemite/hematite mixture) is not obvious in this soil profile (Tables 3 and 7). Maghemite (or maghemite/hematite mixture) seemed to be formed *in situ*. This means that high temperatures due to forest fire may also influence soil mineralogy to a depth of >0.5 m. This finding does not fully agree with the results obtained during an experimental fire where a very rapid decrease with the soil depth (about 45ºC in 2.5 cm soil depth) was observed (Wüthrich *et al.*, 2002). The soil temperature increase caused by fire is short-lived, but the changes induced in soil properties are more or less permanent (Wondafrash *et al.*, 2005). The impact of burning on soil mineralogy may have the potential to cause mineral transformations with moderate (250−500ºC) and severe fires (>500ºC). Maghemite itself can be formed at temperatures as low as 220ºC (Sidhu, 1988) and may revert to hematite at temperatures of ~350ºC (Mullins, 1977). Natural maghemite is, however, often stabilized by impurities giving rise to transformation temperatures exceeding 600ºC (Mullins, 1977; Ketterings *et al.*, 2000). According to Ketterings *et al.* (2000), maghemite was formed (transformation of goethite into maghemite) even at temperatures exceeding 600ºC. Organic matter was necessary (and limiting) for complete conversion of goethite.

A considerable heat transfer can be assumed for the Ascona I site where high SOM contents, and thus material that is potentially available for burning, could be found to a depth of >50 cm. Bioturbation in these soils was not intense enough to explain a possible transfer of maghemite from the soil surface into such a considerable soil depth. Usually, fires occur in forest patches and not in large areas. It is likely that one or more intense burns have affected this site. Ascona I was on a summit position where the heat can 'accumulate' and cause an intense burn. At the Ascona II site, the total including secondary, dithionite-extractable Fe contents

were less and probably beyond the detection limit for Fe phases in oxy-hydroxides by Mössbauer spectroscopy.

Organic matter stabilization

The soils are very rich in organic C and characterized by a black color, compared to other regions in Switzerland. Organic matter could be stabilized by several processes. The formation of organo-metallic complexes is known to strengthen SOM resistance to biodegradation (Bruckert, 1970; Brunner and Blaser, 1989). Kleber *et al.* (2005) suggest that the amount of organic C is preferentially protected in acid soils by interaction with poorly crystalline minerals that is chemically characterized by a ligand exchange between mineral surface hydroxyl groups and negatively charged organic functional groups.

According to the good correlation between Al_p or Fe_p with organic C, accumulation and stabilization of organic matter seems to be promoted by poorly crystalline or organically bound Fe and Al. In the subsoil of all profiles, significant amounts of ITM (allophane and imogolite) were measured. Furthermore, ITM is known to stabilize SOM (*e.g.* Shoji *et al.*, 1993; Basile-Doelsch *et al.*, 2005). This kind of process is frequent in Andosols where non-crystalline Al and humus lead to stable soil aggregates (Shoji *et al.*, 1993; Hanudin *et al.*, 2002; Ugolini and Dahlgren, 2003). In our soils, ITM occurs mainly in the subsoil, so that the role of ITM in organic matter stabilization is of minor importance.

As shown by Denef and Six (2004), the type of clay minerals can affect the macroaggregate formation and stabilization (and consequently organic C). Illite led to stronger organic bonds when compared to kaolinite (Denef and Six, 2004). In our case we found in all topsoils large 2:1 clay minerals contents, *e.g.* vermiculite, HIV or HIS. We presume that these minerals probably helped to establish strong clay–organic matter bonds.

Frequent vegetation burning may produce black carbon that contributes to highly stable organic-matter components in soils (Schmidt and Noack, 2000).

Soil classification

Blaser *et al.* (1997) termed these soils Cryptopodzols, because the eluvial horizon is masked by the dark color of the organic matter. The soils show some similarities to Andosols. According to the WRB (1998), Andosols have a vitric or an andic horizon starting within 25 cm from the soil surface. The diagnostic criteria for an andic horizon are: $Al_o + 1/2Fe_o$ >2%, bulk density <0.9 mg m^{-3}, phosphate retention >70%, clay content >10%, thickness >30 cm and volcanic glass <10%. All diagnostic characteristics of the soil profile Ascona I (except the phosphate retention that was not determined) fulfil the criteria for an Andosol. Regarding Ascona II and Pura, the clay content and also the content of $Al_o + 1/2\ Fe_o$ were too small to meet the andic properties.

The soils had surface horizons rich in organic matter to depths of >50 cm (so-called 'pachic' characteristics; WRB, 1998) and with a low bulk density. A soil showing the properties of a Podzol and an Andosol was described by Kleber *et al.* (2003) in Eastern Saxony, Germany. Those authors suggested the existence of an intermediate pedogenetic pathway between podsolization and andosolization. There was no indication of vertical translocation of metal-organic complexes, but enough evidence to suggest the downward movement of mobile Al/Si phases.

CONCLUSIONS

The soils studied are characterized by an accumulation of organic matter in the upper horizon and by a large content of X-ray amorphous or poorly crystalline Al and Fe phases. These two properties are typical for soils developed on volcanic ash. Only one profile, however, met the andic properties required by the WRB (1998). In all soil profiles, we also observed an early stage of podzolization, where on the one hand the translocation of X-ray amorphous Al and Si seemed to start and on the other the formation of ITM in the subsoil could be detected.

With progressing weathering, mica and chlorite transformed into vermiculite, HIV, HIS or were probably decomposed. Interstratified mica-HIV (or mica-vermiculite) was a typical transitory weathering product of mica transformation into vermiculite. HIS or mica-HIS (as a precursor of smectite) and traces of smectite in the topsoil indicated advanced weathering conditions. Weathering generally resulted in a strong reduction of trioctahedral species and a consequent increase in dioctahedral species. The increase in dioctahedral species was at least partially due to the oxidation of Fe(II) to Fe(III). The presence of maghemite (or maghemite/hematite mixture) in one soil profile indicated that forest fire also influenced the mineral composition. Maghemite was probably derived from ferrihydrite or goethite. The influence of fire was measurable down to the considerable depth of ~50 cm.

ACKNOWLEDGMENTS

This research has been supported by a grant of the Swiss National Science Foundation, nr. 200020-107488/1. We would like to express our appreciation to B. Kägi and D. Giaccai for their assistance in the laboratory. We are, furthermore, indebted to Prof. Heinz Veit and Prof. Helge Stanjek for their helpful comments on an earlier version of the manuscript.

REFERENCES

Basile-Doelsch, I., Amundson, R., Stone, W.E.E., Masiello, C.A., Bottero, J.Y., Colin, F., Masin, F., Borschneck, D. and Meunier, J.D. (2005) Mineralogical control of organic carbon dynamics in a volcanic ash soil on La Réunion. *European Journal of Soil Science*, **56**, 689–703.

Bergmann, J. and Kleeberg, R. (1998) Rietveld analysis of disordered layer silicates. *Materials Science Forum*, **278–281**, 300–305.

Bergmann, J., Friedel, P. and Kleeberg, R. (1998) BGMN – a new fundamental parameters based Rietveld program for laboratory X-ray sources, it's use in quantitative analysis and structure investigations. Commission of Powder Diffraction, International Union of Crystallography. *CPD Newsletter*, **20**, 5–8.

Blaser, P. and Sposito, G. (1987) Spectrofluorometric investigation of trace metal complexation by an aqueous chestnut leaf litter extract. *Soil Science Society of America Journal*, **51**, 612–619.

Blaser, P., Kernebeek, P., Tebbens, L., Van Breemen, N. and Luster, J. (1997) Cryptopodzolic soils in Switzerland. *European Journal of Soil Science*, **48**, 411–423.

Bouchard, M. and Jolicoeur, S. (2000) Chemical weathering studies in relation to geomorphological research in southeastern Canada. *Geomorphology*, **32**, 213–238.

Boudot, J.P., Bel Hadj Brahim, A., Steiman, R. and Seigle-Murandi, F. (1989) Biodegradation of synthetic organometallic complexes of iron and aluminium with selected metal to carbon ratios. *Soil Biology and Biochemistry*, **21**, 961–966.

Bruckert, S. (1970) Influence des composés organique solubles sur la pédogenèse en milieu acide. Thesis, University of Nancy.

Brunner, W. and Blaser, P. (1989) Mineralization of soil organic matter and added carbon substrates in two acidic soils with high non-exchangeable aluminium. *Zeitschrift für Pflanzenernährung und Bodenkunde*, **152**, 367–372.

Burga, C. and Perret, R. (1998) *Vegetation und Klima der Schweiz seit dem jüngeren Eiszeitalter*. Ott Verlag, Thun.

Carcaillet, C. and Talon, B. (2001) Soil carbon sequestration by Holocene fires inferred from soil charcoal in the dry French Alps. *Arctic, Antarctic, and Alpine Research*, **33**, 282–288.

Carnicelli, S., Mirabella, A., Cecchini, G. and Sanesi, G. (1997) Weathering of chlorite to a low-charge expandable mineral in a spodosol on the Apennine mountains, Italy. *Clays and Clay Minerals*, **45**, 28–41.

Dahlgren, R., Shoji, S. and Nanzyo, M. (1993) Mineralogical characteristics of volcanic ash soils. Pp. 101–143 in: *Volcanic Ash Soils; Genesis, Properties and Utilization* (S. Shoji, M. Nanzyo and R. Dahlgren, editors). Developments in Soil Science **21**, Elsevier Science Publishers B.V., Amsterdam.

De Coninck, F., Vasu, A. and Raport, C. (1976) Mineralogy of the clay fraction of 4 soils of the Bucegi Mountains (S. Carpathians-Romania). *Pédologie*, **26**, 255–279.

Denef, K. and Six, J. (2004) Clay mineralogy determines the importance of biological versus abiotic processes for macroaggreggate formation and stabilization. *European Journal of Soil Science*, **56**, 469–479.

Dreher, P. and Niederbudde, E.-A. (2000) Characterization of expandable layer silicates in humic-ferralic cambisols (Umbrept) derived from biotite and hornblende. *Journal of Plant Nutrition and Soil Science*, **163**, 447–453.

Duchaufour, P. (1976) *Atlas Ecologique des Sols du Monde*. Masson, Paris.

EDI (Eidgenössisches Department des Innern), (1992) *Hydrologischer Atlas der Schweiz. Landeshydrologie und -geologie*. Bern, Switzerland.

Egli, M., Mirabella, A. and Fitze, P. (2001) Clay mineral formation in soils of two different chronosequences in the Swiss Alps. *Geoderma*, **104**, 145–175.

Egli, M., Mirabella, A. and Fitze, P. (2003) Formation rates of smectites derived from two Holocene chronosequences in the Swiss Alps. *Geoderma*, **117**, 81–98.

Fanning, D.S., Keramidas, V.Z. and El-Desoky, M.A. (1989) Micas. Pp. 551–634 in: *Minerals in Soil Environment* 2nd edition (J.B. Dixon and S.B. Weed, editors). Soil Science Society of America, Madison, Wisconsin, USA.

Fitze, P., Kägi, B. and Egli, M. (2000) *Laboranleitung zur Untersuchung von Boden und Wasser*. Geographisches Institut der Universität Zürich, Zürich, Switzerland.

Golchin, A., Baldock, J.A., Clarke, P., Higashi, T. and Oades, J.M. (1997) The effects of vegetation and burning on the chemical composition of soil organic matter in a volcanic ash soil as shown by ^{13}C NMR spectroscopy. II. Density fractions. *Geoderma*, **76**, 175–192.

Guillaume, D., Neaman, A., Cathelineau, M., Mosser-Ruck, R., Peiffert C., Abdelmoula, M., Dubessy, J., Villiearas, F., Baronnet, A. and Michau, N. (2003) Experimental synthesis of chlorite from smectite at 300ºC in the presence of iron metal. *Clay Minerals*, **38**, 281–302.

Hantke, R. (1978) *Eiszeitalter 1: Die jüngste Erdgeschichte der Schweiz und ihrer Nachbargebiete. Klima, Flora, Fauna, Mensch, Alt- und Mittelpleistozäne, Vogesen, Schwarzwald, Schwäbische Alb.* Ott Verlag, Thun, Switzerland.

Hantke, R. 1(983) *Eiszeitalter 3: Die jüngste Erdgeschichte der Schweiz und ihrer Nachbargebiete. Westliche Ostalpen mit ihrem bayerischen Vorland bis zum Inn-Durchbruch und Südalpen zwischen Dolomiten und Mont-Blanc.* Ott Verlag, Thun, Switzerland.

Hanudin, E., Matsue, N. and Henmi, T. (2002) Reactions of some short-range ordered aluminosilicates with selected organic ligands. Pp. 319–332 in: *Soil Mineral-Organic Matter – Microorganism Interactions and Ecosystem Health* (A. Violante, P.M. Huang, J.-M. Bollag and L. Gianfreda, editors). Developments in Soil Science, Volume **28A**, Elsevier Science, Amsterdam.

Hossner, C.R. (1996) Dissolution for total elemental analysis. Pp. 49–64 in: *Methods of Soil Analysis, Part 3 Chemical Methods*, (D.L. Sparks, editor). Soil Science Society of America Inc. and American Society of Agronomy Inc., Madison, Wisconsin.

Kaiser, K. and Zech, W. (1996) Defects in estimation of aluminium in humus complexes of podzolic soils by pyrophosphate extraction. *Soil Science*, **161**, 452–458.

Ketterings, Q.M., Bigham, J.M. and Laperche, V. (2000) Changes in soil mineralogy and texture caused by slash-and-burn fires in Sumatra, Indonesia. *Soil Science Society of America Journal*, **64**, 1108–1117.

Kleber, M., Zikeli, S., Kastler, M. and Jahn, R. (2003) An Andosol from Eastern Saxony, Germany. *Zeitschrift für Pflanzenernährung und Bodenkunde*, **166**, 533–542.

Kleber, M., Mikutta, C. and Jahn, R. (2004) Andosols in Germany – pedogenesis and properties. *Catena*, **56**, 67–83.

Kleber, M., Mikutta, R., Torn, M.S. and Jahn, R. (2005) Poorly crystalline mineral phases protect organic matter in acid subsoil horizons. *European Journal of Soil Science*, **56**, 717–725.

Lanson, B. (1997) Decomposition of experimental X-ray diffraction patterns (profile fitting): a convenient way to study clay minerals. *Clays and Clay Minerals*, **45**, 132–146.

Lundström, U.S., van Breemen, N. and Bain, D.C. (2000a) The podzolization process. A review. *Geoderma*, **94**, 91–107.

Lundström, U.S., van Breemen, N., Bain, D.C., van Hees, P.A.W., Giesler, R., Gustafsson, J.P., Ilvesniemi, H., Karltun, E., Melkerud, P.-A., Olsson, M., Riise, G., Wahlberg, O., Bergelin, A., Bishop, K., Finlay, R., Jongmans, A.G., Magnusson, T., Mannerkosky, H., Nordgren, A., Nyberg, L., Starr, M. and Tau Strand, L. (2000b) Advances in understanding the podzolization process resulting from a multidisciplinary study of three coniferous forest soils in the Nordic Countries. *Geoderma*,

94, 335–353.

Luster, J. (1990) Cu(II)-Komplexierung durch gelöstes organisches Material in Wasserextrakten aus Laubstreu sowie durch seine Molekularfiltrations- und Umkehrphasen-Chromatographie-Fraktionen. PhD thesis No 9059, Swiss Federal Institute of Technology, Zürich.

Mailänder, R. and Veit, H. (2001) Periglacial cover-beds on the Swiss Plateau: indicators of soil, climate and landscape evolution during the Late Quaternary. *Catena*, **45**, 251–272.

McKeague, J.A., Brydon, J.E. and Miles, N.M. (1971) Differentiation of forms of extractable iron and aluminium in soils. *Soil Science Society of America Proceedings*, **35**, 33–38.

Mirabella, A. and Sartori, G. (1998) The effect of climate on the mineralogical properties of soils from the Val Genova Valley (Trentino, Italy). *Fresenius Environmental Bulletin*, **7**, 478–483.

Mirabella, A., Egli, M., Carnicelli, S. and Sartori, G. (2002) Influence of parent material on clay minerals formation in podzols of Trentino – Italy. *Clay Minerals*, **37**, 699–707.

Mirabella, A. and Egli, M. (2003) Structural transformations of clay minerals in soils of a climosequence in an Italian alpine environment. *Clays and Clay Minerals*, **51**, 264–278.

Mizota, C. and van Reeuwijk, L.P. (1989) *Clay mineralogy and chemistry of soils formed in volcanic material in diverse climat regions*. International Soil Reference and Information Centre Soil Monograph, vol. 2. Wageningen.

Moore, D.M. and Reynolds, R.C. (1997) *X-ray Diffraction and the Identification and Analysis of Clay Minerals*. 2nd edition, Oxford University Press, New York.

Mullins, C.E. (1977) Magnetic susceptibility of the soil and its significance to soil science: a review. *Journal of Soil Science*, **28**, 233–246.

Murad, E. (1998) Clays and clay minerals study by Mössbauer spectroscopy. *Hyperfine Interactions*, **117**, 39–70.

Nørnberg, P., Schwertmann, U., Stanjek, H., Andersen, T. and Gunnlaugsson, H.P. (2004) Mineralogy of a burned soil compared with four anomalously red Quaternary deposits in Denmark. *Clay Minerals*, **39**, 85–98.

Olis, A.C., Malla, P.B. and Douglas, L.A. (1990) The rapid estimation of the layer charges of 2:1 expanding clays from a single alkylammonium ion expansion. *Clay Minerals*, **25**, 39–50.

Parfitt, R.L. and Childs, C.W. (1988). Estimation of forms of Fe and Al – a review, and analysis of contrasting soils by dissolution and Mössbauer methods. *Australian Journal of Soil Research*, **26**, 121–144.

Parfitt, R.L. and Henmi T. (1982) Comparison of an oxalate-extraction method and an infrared spectroscopic method for determining allophane in soil clays. *Soil Science and Plant Nutrition*, **28**, 183–190.

Righi, D., Girault, P. and Meunier, A. (1986) Transformation des phyllosilicates dans un sol cryptopodzolique humifère du Plateau de Millevaches, France. *Clay Minerals*, **21**, 43–54.

Righi, D., Huber, K. and Keller, C. (1999) Clay formation and podzol development from postglacial moraines in Switzerland. *Clay Minerals*, **34**, 319–332.

Schlumpf, N. (2004) *Schwarze Böden der Südschweiz: organisch-geochemische Charakterisierung einer Toposequenz*. Department of Geography, University of Zurich, Switzerland.

Schmidt, M.W.I., Skjemstad, J.O., Gehrt, E. and Kögel-Knabner, I. (1999) Charred organic carbon in German chernozemic soils. *European Journal of Soil Science*, **50**, 351–365.

Schmidt, M.W.I. and Noack, A.G. (2000) Black carbon in soils and sediments: Analysis, distribution, implications, and current challenges. *Global Biogeochemical Cycles*, **14**, 777–793.

Schroeder, P.A., Melear, N.D., West, L.T. and Hamilton, D.A. (2000) Meta-gabbro weathering in the Georgia Piedmont, USA: implications for global silicate weathering rates. *Chemical Geology*, **163**, 235–245.

Schwertmann, U. (1988) Occurrence and formation of iron oxides in various pedoenvironments. Pp. 267–308 in: *Iron in Soils and Clay Minerals* (J.W. Stucki, B.A. Goodman and U. Schwertmann, editors). D. Reidel, Dordrecht, The Netherlands.

SGK (Schweizerische Geotechnische Kommission) (1967) *Geotechnische Karte der Schweiz.* Blatt Nr. 4 St. Moritz-Bellinzona.

SGK (Schweizerische Geotechnische Kommision) (1974) *Geologischer Atlas der Schweiz 1:25000. Blatt 1313 Bellinzona*.

Shindo, H., Honna, T., Yamemoto, S. and Homna, H. (2002) Distribution of charred plant fragments in Japanese volcanic ash soils with reference to origins of black humic acids. Pp. 466–468 in: *Proceedings of the International Humic Substances Society, 20th Anniversary Conference*. Northeastern University, Boston, MA.

Shoji, S., Nanzyo, M. and Dahlgren, R.A. (1993) *Volcanic Ash Soils – Genesis, Properties and Utilization.* Elsevier, Amsterdam.

Sidhu, P.S. (1988) Transformation of trace element-substituted maghemite to hematite. *Clays and Clay Minerals*, **36**, 31–38.

Skjemstad, J.O., Clarke, P., Taylor, J.A., Oades, J.M. and McClure, S.G. (1996) The chemistry and nature of protected carbon in soil. *Australian Journal of Soil Research*, **34**, 251–271.

Stanjek, H. (1987) The formation of maghemite and hematite from lepidocrocite and goethite in a Cambisol from Corsica, France. *Zeitschrift für Pflanzenernährung und Bodenkunde*, **150**, 314–318.

Tamura, T. (1958) Identification of clay minerals from acid soils. *Journal of Soil Science*, **9**, 141–147.

Tinner, W., Hubschmid, P., Wehrli, M., Ammann, B. and Conedera, M. (1999) Long-term forest fire ecology and dynamics in southern Switzerland. *Journal of Ecology*, **87**, 273–289.

Ugolini, F.C. and Dahlgren, R.A. (2003) Soil development in volcanic ash. *Global Environmental Research*, **6**, 69–81.

Van der Marel, H.W. (1951) Gamma ferric oxide in sediments. *Journal of Sedimentary Petrology*, **21**, 12–21.

Williams, S.T. and Gray, T.R.G. (1974) Decomposition of litter on the soil surface. Pp. 611–632 in: *Biology of Plant Litter Decomposition* (C.H. Dickinson and G.J.F. Pugh, editors). Academic Press, London.

Wondafrash, T.T., Sancho, I.M., Miguel, V.G. and Serrano, R.E. (2005) Relationship between soil color and temperature in the surface horizon of Mediterranean soils: A laboratory study. *Soil Science*, **170**, 495–503.

WRB (1998) *World Reference Base for Soil Resources.* World Soil Resources Reports 84, FAO, Rome.

Wüthrich, Ch., Schaub D., Weber, M., Marxer, P. and Conedera, M. (2002) Soil respiration and soil microbial biomass after fire in a sweet chestnut forest in southern Switzerland. *Catena*, **48**, 201–215.

Zech, W., Guggenberger, P., Zalba, P. and Peinemann, N. (1997) Soil organic matter transformation of Argentinian Hapludolls. *Zeitschrift für Pflanzenernährung und Bodenkunde*, **160**, 563–571.

Zehetner, F., Miller, W.P. and West, L.T. (2003) Pedogenesis of volcanic ash soils in Andean Ecuador. *Soil Science Society of America Journal*, **67**, 1797–1809.

Zoller, H. (1960) Pollenanalytische Untersuchungen zur Vegetationsgeschichte der insubrischen Schweiz.

Denkschrift der Schweizerischen Naturforschenden Gesellschaft, **83**, 45–156.

Zunino, H., Borie, F., Aguilera, S., Martin, J.P. and Haider, K. (1982) Decomposition of ^{14}C-labeled glucose, plant and microbial products and phenols in volcanic ash-derived soils in Chile. *Soil Biology and Biochemistry*, **14**, 37–43.

(*Received 21 February 2006; revised 19 June 2006; Ms. 1147; A.E. Helge Stanjek*)